THE EFFECT OF WINDER TYPE AND WEB MATERIAL PROPERTIES ON WOUND-ON-TENSION

By

Y. Ren, B. Kandadai[1] and J. K. Good
Oklahoma State University
USA

ABSTRACT

The choice of winder type for various web materials has long been a qualitative discussion. Web materials are vast and hence the range of web material properties is also vast. Valid but conflicting opinions for an optimal winder type have been developed from experience bases that represent this vast range of web materials. The purpose of this publication is to quantify how the internal stresses in wound rolls are affected by winder type and web material properties.

INTRODUCTION

Most practical center and all surface winders employ a nip roller, which will allow high speed winding by excluding entrained air into the wound roll. The nip roller also causes the tension in the outer layer of the winding roll to differ from the web tension. This tension in the outer layer of a winding roll is called the wound-on-tension (WOT), which has greater impact on the internal pressure and tangential stresses in wound rolls than all other influences including web material properties. Knowledge of the pressure and tangential stress levels in a wound roll is essential when predicting roll defects. In a center winder with no nip roller the WOT is either equal or less than the web tension T_w due to the tension loss caused by the radial deformation [1].Center and surface winders with impinged nip rollers as shown in Figure 1 complicate the WOT further.

Center winders with a nip roller and surface winders appear very similar. The main difference is whether the torque required to wind a roll is introduced through the core of the winding roll or through a surface driven nip roller. The nip roller can induce slippage between the nip roller and the outer layer and also between the outer layer and the layer beneath. Whenever slippage occurs the slip forces may cause the WOT to be either less or greater than the web tension T_w depending on the direction of the slip forces. The

[1] B. K. Kandadai works as a Mechanical Engineer at Kimberly-Clark Corporation.

WOT is what distinguishes the difference between how center and surface winders will wind a given web.

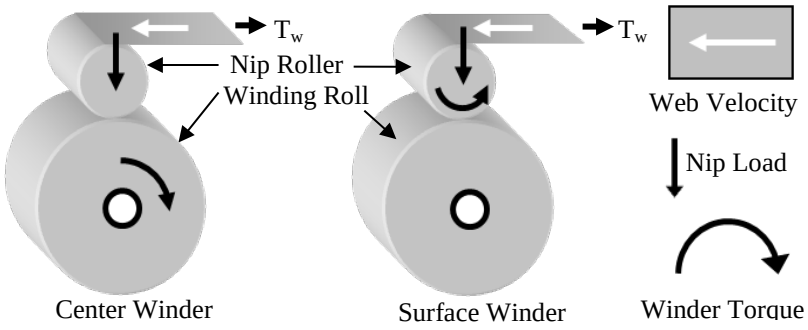

Figure 1 – Winders

Pfeiffer [2] in 1966 was the first to acknowledge that the primary difference between a center winder and all other winders is the influence of the nip roller. He coined a new term "Wound-In-Tension (WIT)", which was the tension in the *current* outer layer of a winding roll, and discussed how this tension was higher than the web tension just upstream of the winder for a roll wound with impinged nip. Pfeiffer [3] then experimentally found that the uppermost layer always slipped in the direction of the rolling nip above the sheets beneath inducing an additional tension in the outermost layer. Rand and Eriksson [4] documented the slippage and tension increase due to impinged nips by applying strain gages to a newsprint web and recording the machine direction strain as the instrumented web was wound into rolls. This work was key in documenting the increases in tension in the outer layer as it passed under the nip roller(s) in the winders. Their work led to a conclusion that the permanent effect of the nip roller on wound roll internal pressures and stresses was primarily due to the slippage induced beneath the outer layer.

Pfeiffer [5] developed the first convenient means of directly measuring the WIT in a roll wound in a surface winder. The method involves extracting the outer web layer away from the surface of the winding roll after the nip and measuring the web tension such that the influence of the nip on the tension in the outer layer could be monitored. Although Pfeiffer's apparatus was setup in a way in which web tension and nip load were not completely independent his findings were still very important.

Good and Fikes [6] studied the pressures in rolls which were center wound with a nip roller. Force sensitive resistors were used to document the pressures in the wound roll after winding was complete. Using a wound roll model in the style of Hakiel [7], the tension in the outer layer in the winding roll was iterated until the model produced pressures of like magnitude to the experimental results. The chief finding in this study was that the WOT was directly affected by web tension prior to the winder and affected through a constant of proportionality to the nip load. The constant appeared to be similar in magnitude to the kinetic coefficient of friction and thus the first WOT algorithm for center winding with an undriven nip roller was generated:

$$\begin{aligned} WOT_{\text{Center Winding with Nip}} &= T_w + \mu_k \frac{N}{h} \text{(stress)} \\ WOT_{\text{Center Winding with Nip}} &= T + \mu_k N \text{ (load per unit width)} \end{aligned} \quad \{1\}$$

where the web tension (T_w) has units of stress or load per unit width (T), the nip load (N) has units of load per unit width of nip contact, and the web thickness (h) has units of length, thus the WOT can have units of stress or load per unit width. Expression {1} was used in place of the web tension as a boundary condition for Hakiel's [7] winding model to produce the internal pressures and circumferential pressures within the wound roll when winding with a center winder with an impinged undriven nip roller. It was proven to work well for winding rolls of polypropylene film and rolls of lightweight coated paper [8] as well as rolls of bond paper [1].

Steves [9] surface wound rolls of newsprint and documented the internal pressure as a function of wound roll radius using pull tabs. He then used a similar method as Good and Fike [6] to back out the WOT. A result from Steve's work was a WOT algorithm for surface winding was:

$$\begin{aligned} WOT_{\text{SurfaceWinding}} &= \mu_k \frac{N}{h} \text{(stress) } N \le 17.5 \text{ N/cm newsprint} \\ WOT_{\text{SurfaceWinding}} &= \mu_k N \text{ (load per unit width)} \end{aligned} \quad \{2\}$$

Later a study by Good, Hartwig, and Markum [10] ascertained how the WOT differed between a center winder with an impinged nip roller and a surface winder and compared results with Pfeiffer [5] and Steves [9] by developing a new WOT apparatus where nip load and web tension were truly independent. They confirmed that when center winding at low nip loads the WOT is well described by expression {1}, at high nip loads the WOT fell below what was predicted by {1} and became less dependent on nip load. When surface winding at low nip levels the WOT was well described by expression {2}. The dependency of WOT on nip load decreased at higher nip load levels and developed some dependency on web tension, which was noted as well by Pfeiffer [5] and Steves [9]. It appeared that the slip behavior given in expressions {1} and {2} was being inhibited at higher nip loads. For a given web the nip load at which expressions {1} and {2} became invalid was unknown without some form of WOT testing in the lab. All the works mentioned above were based on empirical studies.

Modeling the WOT is technically challenging. A schematic is shown in Figure 2 that can represent a center winder (M_{nip}=0), a surface winder (M_{core}=0). Note that the web can slip on the surface of the nip roller. When the web enters the nip contact zone slippage is possible on both the upper and lower surfaces. After exiting the contact zone slippage may occur between the outer web layer and the layer beneath. When that slippage ceases the final value of WOT has been achieved. Modeling however is required to determine the magnitudes and the domain of slippage on the nip surface, in the nip contact zone and on the surface of the winding roll to predict the WOT and the location where the final value is achieved.

Jorkama and von Hertzen [11-13] were the first to achieve a solution of the problem shown in Figure 2 in a reduced form. Their solution focused on a form of the problem in which the web did not wrap the nip roller and they did not allow the slippage between the outer layer and the layer beneath to affect the WOT after exit of the nip contact zone. Their objective was to study the tension in the web at the exit of the contact zone. They applied a modified Panagiotopoulos [14] process to iteratively solve the contact pressures

and the slippage forces on the two contact surfaces and were successful in demonstrating behaviors similar to that shown in [9] and [10]. They were also successful in demonstrating that when higher nip loads were applied that regions of stick behavior began to develop in the contact zone that would cause the WOT to be less than that predicted by expressions {1} and {2}.

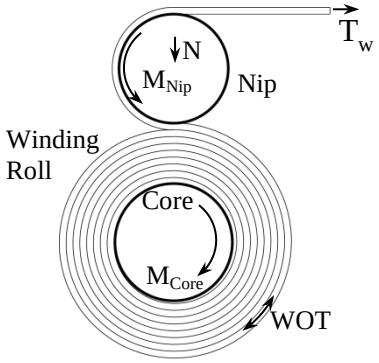

Figure 2 – Model schematic of a center or surface winder

While the work of Jorkama and von Hertzen was a landmark in this field of study there were still gaps in the knowledge regarding prediction of the final value of the WOT. The web material properties were assumed to be constant orthotropic in these studies with only one layer of web compressed between the core and the nip. Pfeiffer [2] noted that the relation between the normal pressure (P) or radial stress (σ_2) and the normal strain (ε_2) appeared logarithmic in the form {3} and the modulus is thus expressed in {4}. Hakiel [7] allowed a form of higher order polynomial {5}, which sometimes provides a more satisfactory correlation to the test data.

{3}

$$E_2 = \frac{d\sigma_2}{d\varepsilon_2} = K_2\left(P + K_1\right) \qquad \{4\}$$

$$E_2 = F_1 + F_2 P + F_3 P^2 + \ldots \qquad \{5\}$$

As layers are wound onto a winding roll pressures increase in the layers that were added earlier as shown by winding models [7]. The layers of web in close proximity to the loaded nip roller are subject to dynamic Hertzian contact pressures. Thus it is known that at least the radial modulus is state dependent on pressure or alternatively on radial strain. Some web and web stack properties are not known well. Jorkama and von Hertzen found that the shear modulus of rigidity ($G_{r\theta}$) was important in determining the stick and slip behavior of the web in the nip and the tension in the web at the exit of the nip. They elected to assume the radial modulus (E_r) and the shear modulus ($G_{r\theta}$) were constants and

tuned them to match one tested WOT value. The tuned material values were then used with their solution method to estimate other WOT. Thus the direct estimation of the final value of the WOT in the outer layer of a winding roll was not possible at that time. That the radial and shear modulus were tuned constants, the unknown impact of the web wrapping the nip roll and whatever additional slippage might occur after the outer layer exited the nip contact zone precluded the direct estimation of WOT.

One objective of this publication will be to demonstrate a robust modeling method that will allow the slippage both before and after the nip contact zone to affect the final value of the WOT. A second objective will be to demonstrate how the state dependency of web material properties can be measured and included in modeling. The last objective will be to demonstrate how the modeling method can distinguish how winder type and web material properties can impact the final value of the WOT.

DEVELOPMENT OF EXPLICIT FINITE ELEMENT WINDING MODELS

Winding process with a nip roller has complex contact situations where the web contacts the nip roller surface, the nip roller and the web layer beneath in the nip contact zone and finally itself as the web winds onto the wound roll. The amount of contact is increasing as successive layers wind onto the wound roll. The explicit method is usually preferred over implicit methods in simulating this kind of problems. In the explicit method the displacements, velocities and accelerations are obtained via information known from the previous time increments. Neither iteration nor convergence checking is required. This guarantees the method to be robust while implicit methods, solving in an iterative way, have difficulty in achieving convergence.

The web, a nip roller and a core, as shown in Figure 2 were modeled in Abaqus/Explicit. The base web material modeled in this study was an oriented Polyester. The nip roller and the core are modeled with rigid surfaces in Abaqus to save computational cost. Based on the consideration of solution accuracy (by eliminating numerical deficiencies such as shear locking and hour glassing) and computational cost, a mesh consisting of four-node quadrilateral reduced integration plane strain elements (CPE4R in Abaqus) with the size of 0.635×0.085 mm was used. Three such elements (Figure 3b) were used through the thickness of the web to capture bending effects.

To model the center winding condition, the loading procedure in Abaqus/Explicit was divided into three steps: pretension, nip loading and winding. In the pretension step shown in Figure 3a, the leading end of the incoming web layer is tied to the core in a small area, while the core and nip roller are restrained all DOFs. The lower end point on the right end surface of the web is restrained to only have horizontal displacement. A constant winding tension T_w is prescribed at the right end surface of the web and is maintained during the simulation. In the nip loading step shown in Figure 3b, the 2-DOF of nip roller is released. A vertical downward concentrated force representing the nip load N was applied at the central reference node of the nip roller and was maintained during the simulation. All other loads and BCs are inherited from the previous step. In the winding step shown in Figure 3c, the rotation of the core about the 3 axis is released and an angular velocity ω is assigned. Other loads and BCs remain identical. Modeling surface winding was very similar except the angular velocity in Figure 3c was now input to the nip roller and core/wound roll was free to rotate.

In Figure 3 the potential for surface interaction is shown between the web and the nip, the web upon the core and self-contact of the web winding upon itself. Contact pair with penalty method is used to model the web-core and web-nip interactions. Self-contact with kinematic method is used to model web-web interactions [15]. The friction between

all contacting surfaces is modeled using Coulomb's friction. In this model, two contacting surfaces can react shear stresses up to a certain magnitude across their interface prior to slipping relative to one another, in a state is known as stick. After the sliding of surfaces starts the critical shear stress (τ_{crit}) is defined as a fraction of the contact pressure (p(x)) between the surfaces per expression {10}:

$$\begin{aligned} \tau_{crit} &< \mu p(x) \Rightarrow \text{stick} \\ \tau_{crit} &= \mu p(x) \Rightarrow \text{slip} \end{aligned} \qquad \{10\}$$

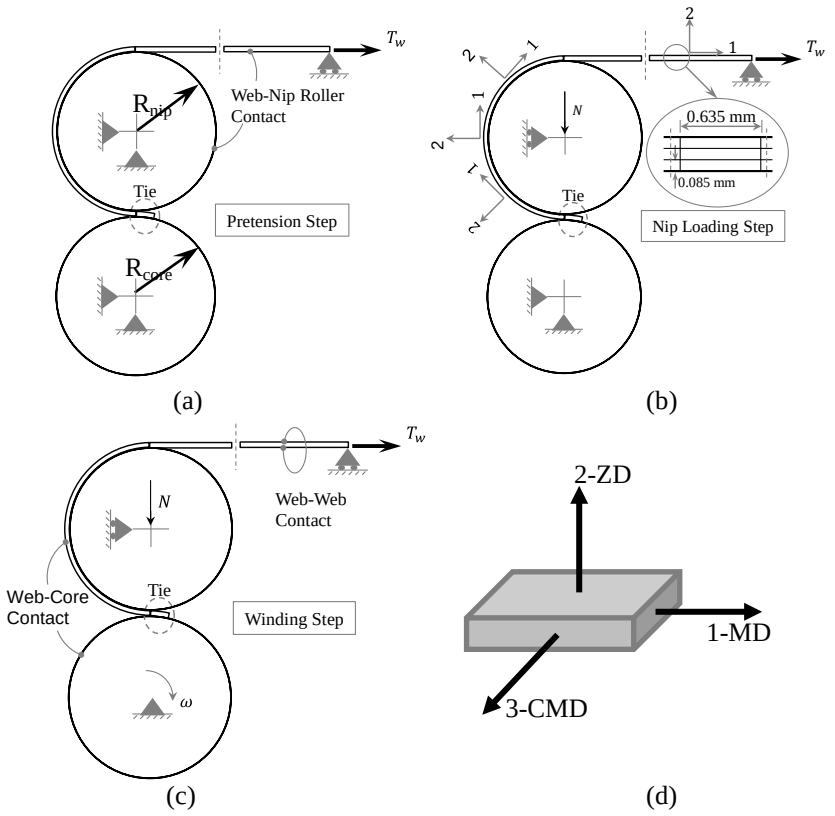

Figure 3 – Modeling steps for center winding using Abaqus/Explicit

CENTER VERSUS SURFACE WINDING: CONSTANT ORTHOTROPIC WEB PROPERTIES: HIGH MD MODULUS

The first focus will be for high modulus materials that would encompass many grades of paper and some plastic films such as polyester. The web modeled is 254 μm thick and 15.24 cm wide. In these simulations the radius of the nip (R_{nip}) and the core (R_{core}) were 5.08 and 4.29 cm, respectively. The friction coefficient in all contact interactions were set at 0.3. The 1, 2 and 3 material property directions are related to the machine direction (MD), radial z direction (ZD) and cross machine direction (CMD) shown in Figure 3b and 3d. Assumptions of plane strain and constant orthotropic web properties were made initially. The orthotropic material properties needed for plane strain

analyses in the 1-2 plane are shown in the constitutive expressions {11} with $\varepsilon_{33}=0$. Orthotropic material model is symmetric requiring Maxwell-Betti reciprocity theorem {12}. This reduces the number of independent material properties to seven. The properties used in this investigation are shown in Table 1. As discussed earlier the radial modulus E_2 is state dependent on pressure. An average value of E_2 was selected for the range of nip loads studied. The constant value of G_{12} came from an approximation made originally by St. Venant [16]. Later these constant values will be allowed to vary.

$$\begin{Bmatrix} \varepsilon_{11} \\ \varepsilon_{22} \\ \varepsilon_{33} \\ \gamma_{12} \end{Bmatrix} = \begin{bmatrix} 1/E_1 & -\nu_{21}/E_2 & -\nu_{32}/E_3 & 0 \\ -\nu_{12}/E_1 & 1/E_2 & -\nu_{23}/E_2 & 0 \\ -\nu_{13}/E_1 & -\nu_{23}/E_2 & 1/E_3 & 0 \\ 0 & 0 & 0 & 1/G_{12} \end{bmatrix} \begin{Bmatrix} \sigma_{11} \\ \sigma_{22} \\ \sigma_{33} \\ \tau_{12} \end{Bmatrix} \qquad \{11\}$$

$$\nu_{12}/E_1 = \nu_{21}/E_2, \; \nu_{13}/E_1 = \nu_{31}/E_3, \; \nu_{23}/E_2 = \nu_{32}/E_3 \qquad \{12\}$$

E_1	E_2	E_3	ν_{12}	ν_{13}	ν_{23}	G_{12}
4.89 GPa	47.2 MPa	5.10 GPa	0.3	0.36	0.01	16.3 MPa

Table 1– Constant Orthotropic Properties for High In-Plane Modulus Simulations

Low Nip Load Behavior

The web tension for the web entering the winder (T_w) was set at 2.07 MPa and the nip load was 26.3 N/cm for the simulations that produced the following results. The web machine direction (MD) stresses are considered first in Figure 4. These stresses were determined by averaging the MD stresses through the thickness of the web. The stresses in Figure 4 are shown at the conclusion of the winding simulation where the entire web modeled is now in the form of a spiral in the wound roll. The results are presented versus a curvilinear MD coordinate. The origin of this coordinate system is near the entry of the nip contact zone. A negative MD coordinate refers to web prior to or in contact with the nip roller. The objective is to study the WOT in the outer layer and the results for MD coordinates in the range of -20 to 20 cm are of most interest. The spike in MD stress at 27 cm is of consequence and will be discussed later. The positions of the spikes at 27, 56, 80 and 109 cm would have fallen on a radius of the wound roll beneath the nip roller at the completion of the simulation.

In Figure 5 the MD membrane stresses are shown for a smaller range of the abscissa from Figure 4. Prior to entry of the nip roller the free web is shown to exhibit the set level of web tension (T_w=2.07 MPa). As the web transits the surface of the nip roller the MD membrane stresses exponentially decay as a result of slippage. Using the capstan slippage expression the MD stress prior to the entry of the nip contact zone should be:

$$T_{\text{entry contact zone}} = \frac{T_w}{e^{\mu\theta}} = \frac{2.07}{e^{0.3\pi}} = 0.81\,\text{MPa} \qquad \{13\}$$

where θ is the angle of wrap and μ is the friction coefficient. This is very near the computed value of stress for both center and surface winding seen at the entry of the nip contact zone in Figure 5. Large increases in membrane stress are witnessed in the nip contact zone. After exiting the nip contact zone only modest changes in MD stress occur and the final value of WOT is witnessed. Note that the WOT for center winding is nearly 2 MPa larger than for surface winding, which is equal to the web tension of 2.07 MPa.

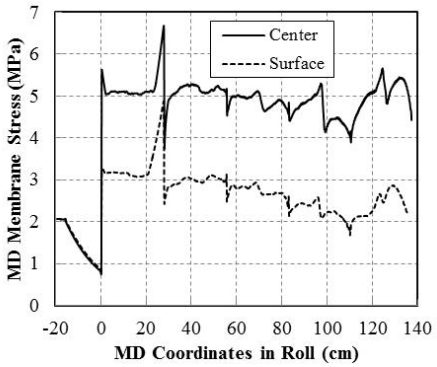

Figure 4 – Machine direction membrane stress in the web (N=26.3 N/cm)

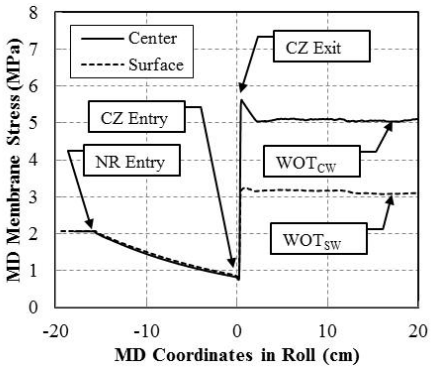

Figure 5 – MD membrane stresses and the WOT (T_w=2.07 MPa, N=26.3 N/cm)

The largest changes in MD stress which affected the final WOT values in both center and surface winding occurred in the nip contact zone as shown in Figure 5. To examine what caused these changes the contact shear stresses are shown in Figure 6 superimposed on the envelopes of the critical levels of shear stress required to induce slippage (τ_{crit}). Note the contact shear stresses never exceed the critical shear stresses. When the contact shear stress reaches the critical shear stress slippage will result. In cases where the contact shear stress is less than the critical value stick behavior will result. Slip is occurring through the entire contact zone on the lower surface for both center and surface winding as shown in Figure 6b. The lower surface is in contact with the previous layer that was wound onto the roll. The behavior on the upper surface however is markedly different with slip occurring near the entry and exit but separated by a zone of stick. It is also evident that the contact shear stresses differ between center and surface winding on the upper surface. The upper web surface is in direct contact with the surface of the nip

roller. Equilibrium can be established for the web in the contact zone if the contact shear stresses are integrated on the upper and lower surfaces as shown in Figure 7.

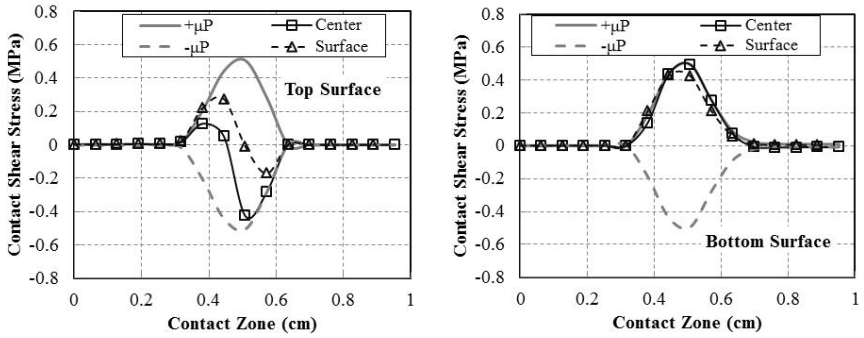

(a) (b)

Figure 6 – Contact shear stresses on the top web surface (a) and the bottom web surface (b) in the contact zone (T_w=2.07 MPa, N=26.3 N/cm)

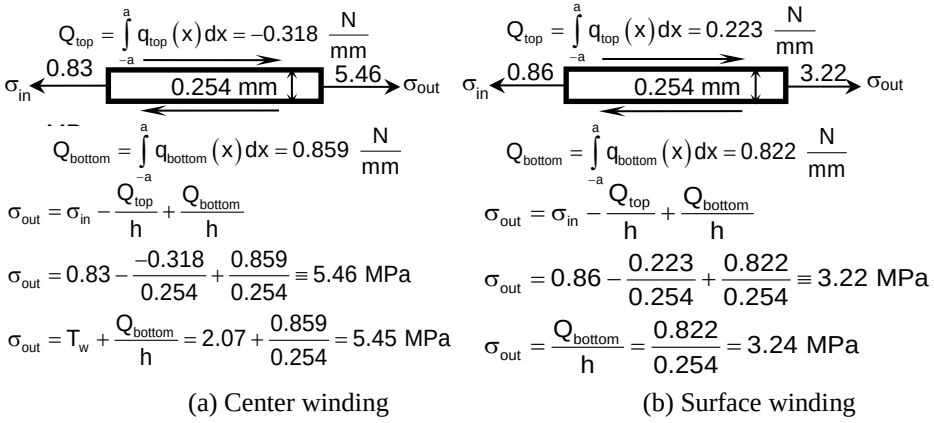

(a) Center winding (b) Surface winding

Figure 7 – Equilibrium of web in contact zone (T_w=2.07 MPa, N=26.3 N/cm)

Now the difference between center and surface winding becomes quantifiable. The major difference is the sign and magnitude of the shear traction on the upper surface of the web in the contact zone. It is this difference which is responsible for the majority of the 2.24 MPa difference in σ_{out}, which is approximately the value of the web tension (T_w) 2.07 MPa. This is consistent with what the empirically derived expressions {1} and {2} forecast as the difference in WOT between center and surface winding.

Why this difference occurs is difficult to understand when considering how similar the values of σ_{in} were for both center and surface winding as demonstrated in Figures 5 and 7. If equilibrium is considered on another scale, as shown in Figure 8, this difference can be explained. Equilibrium of the web on the surface of the nip roller prior to the nip contact zone and the equilibrium for the web in the contact zone are expressed in {14} and {15}:

$$\sigma_{in} = T_w - \frac{Q_{wrap}}{h} \qquad \{14\}$$

$$\sigma_{out} = \sigma_{in} - \frac{Q_{top}}{h} + \frac{Q_{bottom}}{h} \qquad \{15\}$$

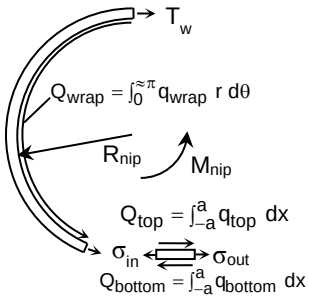

Figure 8 – Equilibrium of the web on the nip roller and in the contact zone

For center winding, the torque applied to the nip (M_{nip}) is zero. The applied surface tractions acting on the nip roller must be in equilibrium:

$$Q_{top}R_{nip} + Q_{wrap}R_{nip} = 0 = M_{nip} \qquad \{16\}$$

For center winding the MD stress at the exit to the contact zone is found by inserting expressions {14} and {16} into {15}:

$$\sigma_{out} = \sigma_{in} - \frac{Q_{top}}{h} + \frac{Q_{bottom}}{h} = \left(T_w - \frac{Q_{wrap}}{h}\right) - \frac{-Q_{wrap}}{h} + \frac{Q_{bottom}}{h} = T_w + \frac{Q_{bottom}}{h} \qquad \{17\}$$

For surface winding, the torque (M_{nip}) will be approximately the web tension, in units of force, multiplied by the radius of the nip (R_{nip}). Again the applied surface tractions acting on the nip roller must be in equilibrium with the applied torque:

$$Q_{top}R_{nip} + Q_{wrap}R_{nip} = M_{nip} = T_w h R_{nip} \qquad \{18\}$$

For surface winding the MD stress at the exit to the contact zone is found by inserting expressions {14} and {18} into {15}:

$$\sigma_{out} = \sigma_{in} - \frac{Q_{top}}{h} + \frac{Q_{bottom}}{h} = \left(T_w - \frac{Q_{wrap}}{h}\right) - \left(\frac{T_w h - Q_{wrap}}{h}\right) + \frac{Q_{bottom}}{h} = \frac{Q_{bottom}}{h} \qquad \{19\}$$

Comparison of expressions {17} and {19} shows that the MD stress at the exit to the contact zone is higher by a value of the web tension T_w for center winding than in surface winding. Results from expressions {17} and {19} are shown in Figures 7a and 7b which compare quite well with the MD stress at the exit of the contact zone σ_{out} computed by Abaqus. Expressions {17} and {19} become expressions {1} and {2} when the lower

contact surface is void of stick behavior and for cases where there is little change in the membrane stress after the web exits the nip contact zone, then σ_{out} approaches the WOT.

High Nip Load Behavior

The web tension for the web entering the winder (T_w) remained at 2.07 MPa and the nip load was increased to 109.5 N/cm for the simulations that produced the following results. The MD membrane stresses are shown in Figure 9 for web just entering the nip roller, wrapping the nip roller, passing through the nip contact zone and exiting to become the outer layer in the winding roll.

There is some similarity of the stresses presented in Figure 9 with those shown in Figure 5 but the nip load increasing over four times has caused some differences. The WOT has increased significantly for both center and surface winding cases. Note how the MD stresses continue to increase after the web exits the contact zone. The peak values that correspond to the WOT occur almost 10 cm beyond the exit of the nip contact zone.

The contact shear stresses are shown in Figure 10 which can be compared to the lower nip load results in Figure 6. With the higher nip load larger contact pressures are developed. The contact shear stresses in Figure 10 are considerably larger than those in Figure 6. Note that a large zone of stick behavior occurs on the bottom surface in Figure 10b whereas in Figure 6b the lower surface is exhibiting slip throughout the contact zone.

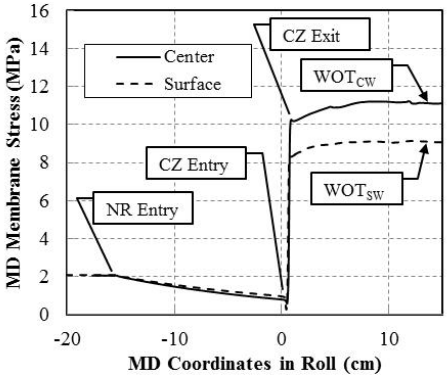

Figure 9 – MD membrane stresses and the WOT (T_w=2.07 MPa, N=109.5 N/cm)

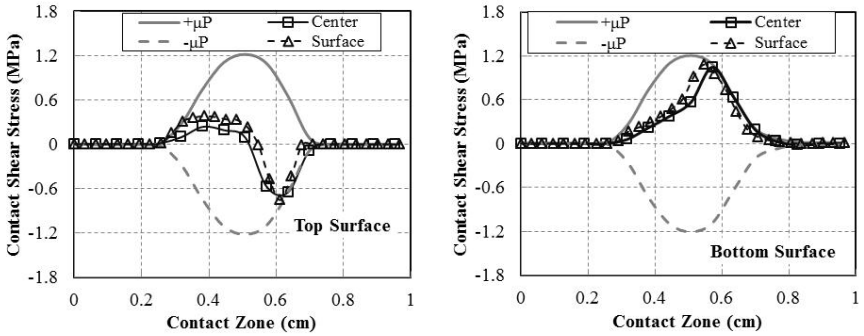

(a) (b)

Figure 10 – Contact shear stresses on the top web surface (a) and the bottom web surface (b) in the contact zone (T_w=2.07 MPa, N=109.5 N/cm)

The Impact of Nip Loads and Web Tension on WOT

In the preceding sections the MD stresses at the exit of the contact zones (σ_{out}) have been studied. For low nip loads the stress at the exit of the contact zone may be very close to the WOT as shown in Figure 5. For a high nip load the highest MD stress and hence the WOT occurred after exiting the contact zone as shown in Figure 9. The WOT for several nip load levels are shown in Figure 11 in units of load per unit width. This is obtained by taking the product of the WOT in units of stress times the web thickness h. Results are shown for web tensions of 2.07 MPa (5.25 N/cm) and 6.89 MPa (17.5 N/cm).

With WOT and nip load in like units the results of the Abaqus/Explicit computations can be compared directly to the WOT expressions {1} and {2} that were empirically derived. At lower nip load levels the slope of the center and surface winding results are very close to 0.3, the friction coefficient used in these analyses. The agreement between expressions {1}, {2} and the Abaqus results is quite good at low nip loads. The stick behavior on the lower surface of the contact zone causes the Abaqus results to be lower than predicted by expressions {1} and {2} at higher nip loads. The Abaqus/Explicit results capture the behavior of the measured WOT results that were shown in [9] and [10]. Note that web tension has a negligible effect on WOT when surface winding which agrees in form with expressions {2} and {19}. Web tension is shown to affect the WOT in center winding in Figure 11.

Use of expressions {1} or {17} would predict a constant WOT difference of 12.25 N/cm between the WOT developed at web tensions of 5.25 and 17.5 N/cm. From Abaqus the difference in WOT begins at 12.75 N/cm at a nip load of 26.3 N/cm and decreases to a difference of 7.7 N/cm at a nip load of 109.5 N/cm. The Q_{top} and Q_{bottom} terms that entered the discussion of equilibrium in expression {15} were integral in deriving expressions {17} and {19}. The Q_{top} and Q_{bottom} terms may have a dependency on the winding tension (T_w). Although this dependency is small here for surface winding (Figure 11) it is significant for center winding.

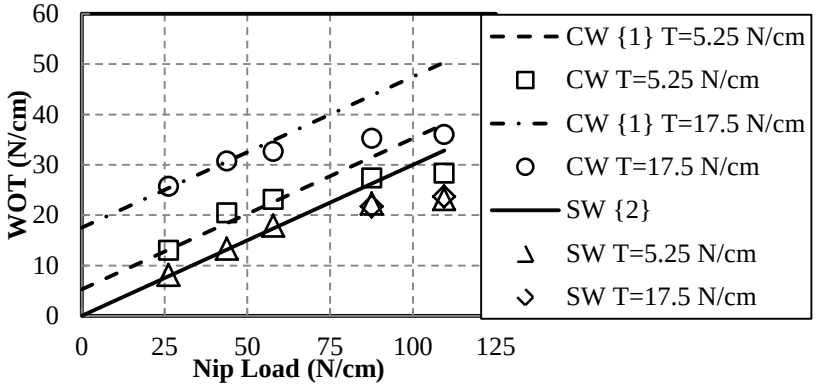

Figure 11 – The WOT for center (CW) and surface (SW) winding per expressions {1} and {2} and from Abaqus/Explicit (discrete data) for a high in-plane modulus web

CENTER VERSUS SURFACE WINDING: CONSTANT ORTHOTROPIC WEB PROPERTIES: LOW IN-PLANE MODULUS

The impact of a low in-plane modulus on WOT is significant. Additional explicit analyses were conducted where all properties remained the same per Table 1 except the

MD and CMD modulus as shown in Table 2. This modulus is similar to what might be expected for a tissue, non-woven or a low density polyethylene web.

E_1	E_2	E_3	ν_{12}	ν_{13}	ν_{23}	G_{12}
138 MPa	47.2 MPa	138 MPa	0.3	0.3	0.01	16.3 MPa

Table 2 – Constant Orthotropic Properties for Low In-Plane Modulus Simulations

The MD membrane stresses in the vicinity of the nip contact zone are shown in Figure 12 for two web tensions and a nip load of 87.6 N/cm. These can be compared to the MD membrane stresses for high in-plane modulus webs in Figure 5. One apparent difference is that prior to the nip contact zone entry the MD membrane stress is essentially that of web tension (T_w). Thus the slippage of the web that wrapped the nip roller that was witnessed for high in-plane modulus webs in Figure 5 is much reduced for the low in-plane modulus web in Figure 12. After the exit of the contact zone the MD membrane stresses become very uniform and the final value of the WOT is attained shortly after the web exits the contact zone. Also note that for the two surface winding results shown that the MD membrane stress and hence the WOT is now affected by web tension. Thus very different behaviors are witnessed for the low in-plane modulus webs than were previously witnessed for the high in-plane modulus webs.

The majority of the difference witnessed is due to the slip behavior in the contact zone. This can be examined in Figure 13 for both center and surface winding cases for a web tension (T_w) of 4.14 MPa and a nip load of 87.6 N/cm. Note that large zones of stick behavior are witnessed by the web on both the top and bottom surfaces. If this slippage is compared to that for the high in-plane modulus webs that were presented in Figures 6 and 10 it can be noted that the stick behaviors witnessed in Figures 13a and 13b are occurring over a larger portion of the contact zone than even for the high nip load results shown in Figure 10. The difference is that these zones of stick behavior become established at much lower nip loads for the low in-plane modulus webs.

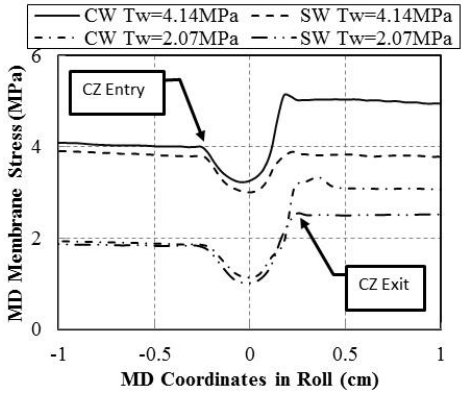

Figure 12 – MD membrane stresses and WOT for a low modulus web (N=87.6 N/cm)

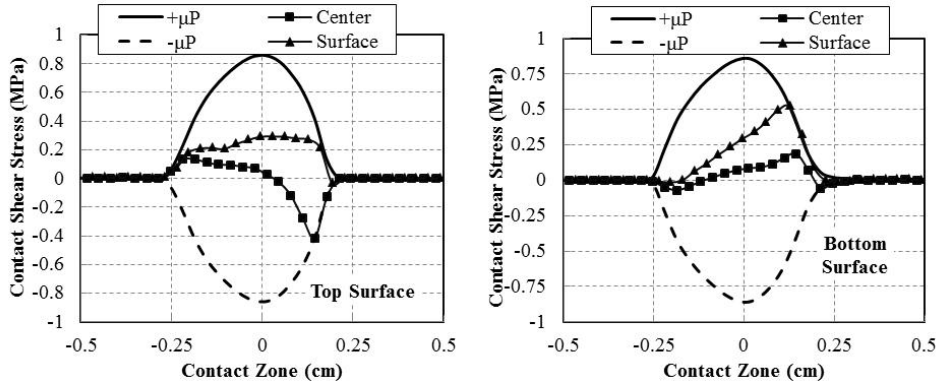

Figure 13 – Contact shear stresses for a low in-plane modulus web on the top web surface (a) and the bottom web surface (b) in the contact zone (T_w=4.14 MPa, N=87.6 N/cm)

Figure 14 shows a comprehensive result of WOT for low in-plane modulus web. Center and surface winding at two web tensions 2.07 MPa (5.25 N/cm) and 4.14 MPa (10.5 N/cm) and related empirical and analytical solutions are shown. For center winding Abaqus results bare little comparison to expression {1} except at the smallest nip load. The WOT appears to be almost independent of nip load for the center winding cases. For surface winding there is some dependency on nip load which would compare with expression {2} at the lowest nip loads. At higher nip loads the dependency on nip load declines and now the WOT appears to be affected by web tension (compare results for T=5.25 and 10.5 N/cm) which is not a behavior that is consistent with expression {2}.

As shown in Figure 12 the MD membrane stress at the exit of the contact zone (σ_{out}) is close to the final value of the WOT in the outer layer of the winding roll. If the equilibrium expressions {17} and {19} generated earlier are recast in units of load per unit width by multiplying by the web thickness h:

$$WOT_{CW} \approx \sigma_{out} h = T_w h + Q_{bottom} = T + Q_{bottom} \quad \{20\}$$

$$WOT_{SW} \approx \sigma_{out} h = Q_{bottom} \quad \{21\}$$

Comparison of the estimate of the WOT for center winding {20}, surface winding {21}, and the final value of WOT are also shown in Figure 14. For center winding observe that over the range of nip load in Figure 14 that Q_{bottom} is not large and does not vary much with respect to nip load. For the two winding tensions shown the WOT is affected more by web tension than by nip load. For surface winding note at lower nip loads the WOT behavior becomes similar to that given by expression {2}. Again the results that show the WOT is affected by web tension (T) are not consistent with expression {2}. Through expression {21} it is apparent that the WOT is influenced by web tension (T) but by affecting Q_{bottom}. Expressions {20} and {21} are approximations for the final value of the WOT. The expressions through equilibrium should exactly predict the web tension at the exit of the contact zone. While simplistic in form expressions {20} and {21} both rely upon knowledge of Q_{bottom}. To determine Q_{bottom} requires the contact mechanics analyses which in this case were performed using Abaqus/Explicit. The explicit analyses also determine if there will be additional slippage

between the outer layer and the layer beneath after the exit of the nip contact zone which will affect the final value of the WOT.

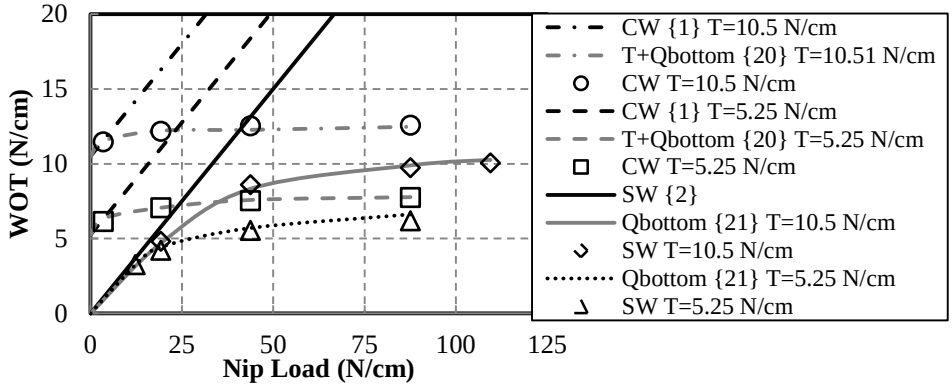

Figure 14 – WOT for center (CW) and surface (SW) winding per expressions {1} {2} {20} and {21} and from Abaqus/Explicit (discrete data) for a low in-plane modulus web

STATE DEPENDENT WEB MATERIAL PROPERTIES

It has been well documented that some orthotropic web properties are constant for many webs, the MD and CMD modulus for example. Other properties are not well documented. The purpose of this section is to fully document the properties of the 254 μm polyester web. These properties will be used in simulations and then compared to test data in a following section. Seven material constants will be needed to fully define an orthotropic web material undergoing plane strain analysis.

The in-plane moduli for the polyester web were measured using procedures consistent with ASTM D882-12 [17]. The machine direction E_1 and cross-machine direction E_3 modulus of the film were measured at 4895 MPa and 5102 MPa, respectively. To determine the radial direction E_2 compression tests were conducted on a 2.54 cm high stack of web coupons that were cut into 15.2 × 15.2 cm^2 squares. The experimental pressure-strain behavior is fitted with Pfeiffer's expression {3}. A least squared error routine was used to provide the best possible fit to the test data. The least error resulted when K_1 and K_2 were 3.45 KPa and 120, respectively. With K_1 and K_2 determined the radial modulus could be formed {4}:

$$E_2 = 120\left(P + 0.00345\right)\text{MPa} \qquad \{22\}$$

where P is the contact pressure in units of MPa

A value of the in-plane Poisson ration ν_{13} was taken at 0.36, consistent with tests conducted using ASTM D638-10 [18, 19]. The Poisson ratios ν_{12} and ν_{32} were not evident in the literature and a test was devised. A web was subjected to a tensile strain in the machine direction ε_1 in a material testing system. The strain was measured in the 2 direction by measuring the change in capacitance between the two precision ground aluminum plates in Figure 15. The plates were held in contact with the web with light clamping pressure. For a parallel plate capacitor the capacitance is:

$$C = \frac{\varepsilon_0 kA}{h} \qquad \{23\}$$

where ε_o is the permittivity of space (8.854×10^{-12} F/m), k is the dielectric of polyester (taken as 3 for polyester [20]), A is the area of the aluminum plates and h is the separation of the plates. Expression {23} can be rearranged to infer the web thickness h which will decrease as the strain in the machine direction strain increases. The strain in the 2 direction can then be inferred from the measured changes in capacitance:

$$\varepsilon_2 = \frac{h_1 - h_0}{h_0} = \frac{C_1 - C_0}{C_0} \qquad \{24\}$$

where h_0 and h_1 are the unstrained web thickness and the deformed web thickness at an MD strain ε_1. C_0 and C_1 are the capacitances measured when the web was unstrained and then strained in the MD at level ε_1, respectively. The results of such a test are shown in Figure 15. The slope is reasonably constant considering the friction that is involved in the test. For a web subject to uniaxial stress in the MD, ν_{12} can be determined from the slope which is approximately 0.37. ν_{32} was also taken as 0.37.

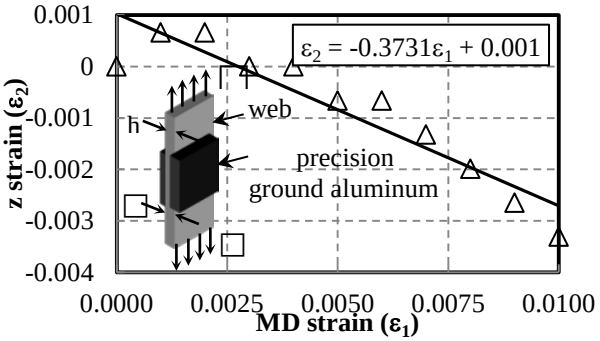

Figure 15 – Test Setup and Strain Data Used to Discern ν_{12}

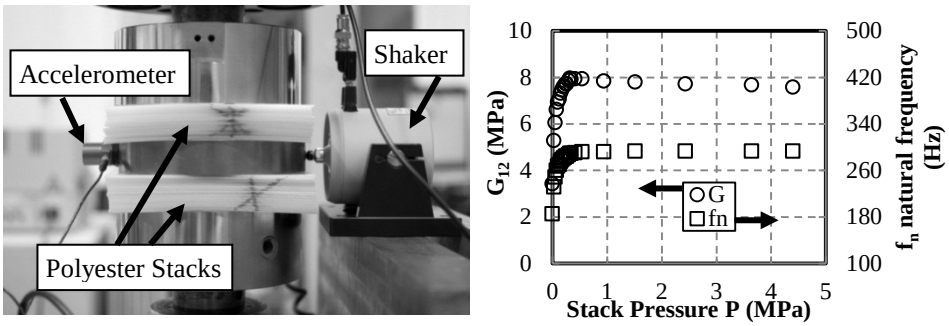

(a) (b)

Figure 16 – Shear modulus G_{12} test setup (a) and G_{12} inferred from natural frequency (b)

To determine G_{12} two stacks of web were subjected to set levels of pressure by a material testing system. An electromagnetic shaker harmonically oscillated a steel platen

which subjected the web stacks in compression to an oscillatory shear as shown in Figure 16a. The frequency of oscillation input to the shaker was varied slowly until an accelerometer on the opposite side of the platen produced peak output. When this peak was found it was known that the system composed of the web stacks and the steel platen were oscillating at the first natural frequency in shear. This natural frequency is related to the shear modulus. Thus measurement of the natural frequency allowed the inference of the shear modulus. This setup can be modeled as a single degree of freedom dynamic system:

$$G_{12} = \frac{2\pi^2 f_n{}^2 H}{A}\left(M + \frac{2}{3}m\right) \qquad \{25\}$$

where f_n is the natural frequency (Hz), H is the height of each web stack and A is the area of the stack, M is the mass of the platen and m is the mass of each of the web stacks, which are assumed identical. Results for the polyester web are shown in Figure 16b. Thus the shear modulus is shown to be highly dependent on stack pressure when stack pressure is low but becomes nearly constant at high stack pressure.

All of the material parameters required for the plane strain analysis of a polyester web have been determined and are shown in Table 3. The moduli of elasticity, the shear modulus and the contact pressure P all have units of MPa. Any properties that are state dependent on pressure require the pressure to be input in units of MPa.

E_1	E_2	E_3	ν_{13}	ν_{12}	ν_{32}
4895	120(P+0.00345)	5102	0.36	0.37	0.37
G_{12}			ν_{31}	ν_{21}	ν_{23}
P<0.23: 15.54P+4.81	P>0.23: 7.8		0.38	$9.07*10^{-3}$(P+.00345)	$8.7*10^{-3}$(P+.00345)

Table 3 – State Dependent Material Properties for a 254 μm Web

MODELING CENTER WINDING WITH STATE DEPENDENT WEB MATERIAL PROPERTIES IN ABAQUS/EXPLICIT

The modeling of winding is identical to that described earlier in the section on modeling. But in this section material properties are allowed to be state dependent. Abaqus/Explicit allows users to define how the material properties are updated in a Fortran subroutine entitled VUMAT. Since the pressure range within web material in the nip winding process is high it is important to model the state dependency of material properties. Material properties in Table 3 were implemented in a VUMAT subroutine.

Winding experiments were conducted on and instrumented winder shown in Figure 17. The winder was fitted with additional rollers and load cells which allowed the measurement of σ_{out}. The winder parameters are shown in Table 4.

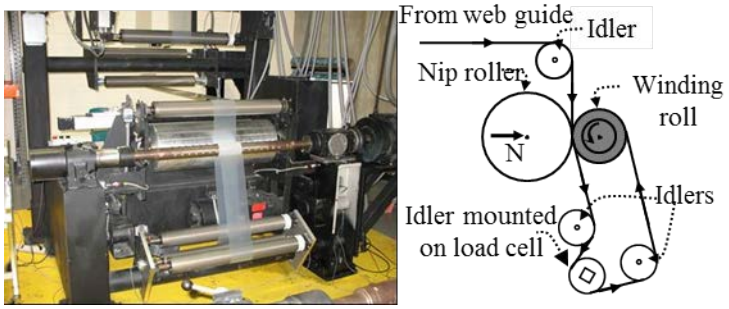

Figure 17 – Center Winding Verification Tests Conducted on 254 μm Polyester

h	R_{core}	R_{nip}	$\mu_{n/w}$	$\mu_{w/w}$	$\mu_{c/w}$	ω_{core}
0.0254 cm	4.43 cm	12.7 cm	0.18	0.16	0.18	3 rad/s
T_w	N					
5.25 N/cm	43.8, 58.4, 87.6, 109, 146, 193 N/cm					

Table 4 – Center Winder Setup Parameters

The results of the winding tests and the Abaqus simulations are shown in Figure 18. The agreement between the simulations, the test data and the center winding algorithm {1} is quite good at lower nip loads. At higher nip loads (100-200 N/cm) the simulations and the test data show larger zones of stick forming on the lower surface of the web, similar to that shown in Figure 10b which limits the WOT to be less than that given by expression {1}. There is some discrepancy at the higher nip loads between the test values of WOT and those harvested as discussed earlier from the Abaqus simulations. This discrepancy can be partially resolved by considering that the outer layer had to be pulled away from the surface of the winding roll to make the WOT test measurement as shown in Figure 17. The Abaqus modeled the case where the outer layer remains in contact with the winding roll as shown in Figure 2. Thus the friction conditions between the outer lap and the layer beneath are very different for the simulations than existed in the tests.

The simulations show that the slippage between the outer lap and the layer beneath are important in determining the final value of the WOT. In Figure 4 a spike in MD membrane stress was shown at 27 cm. This spike was the result of slippage that was occurring beneath the outer lap just prior to the outer layer becoming the second layer. The nip roller was inducing slippage beneath the outer layer and the layer beneath in the nip contact zone. This occurred in the simulations which the web properties were allowed to be state dependent as well. In Figure 19a the tension in the outer lap is shown for the case in which the nip load was 193 N/cm. The tension rises rapidly at the left of the chart where the web passed through the nip contact zone the first time. Note the rise in MD web tension at approximately 80 cm just prior to the outer lap entering the nip contact zone again. This is due to slippage which is shown in Figure 19b. Note that the contact shear stresses become equal to the friction limit prior to the outer layer entering the nip contact zone the second time at an MD coordinate of 80 cm. It was concluded that it was more appropriate to use the average of the MD tension in the outer lap between the exit and the entry of the contact zone shown in Figure 19a. This average was calculated for all nip load cases in the simulations and the results are shown in Figure 18. These averages compare much better with the test values of WOT at the higher nip load levels.

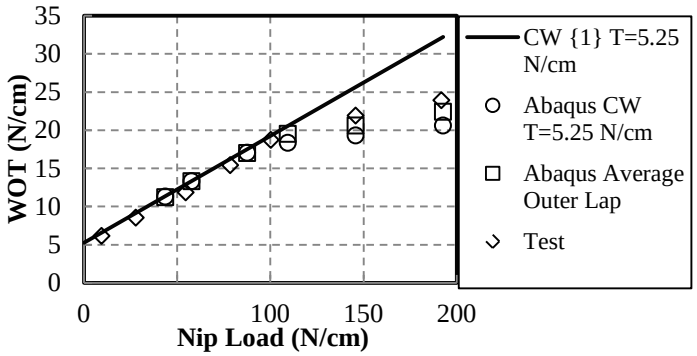

Figure 18 – WOT for Center Winding 254 μm Polyester

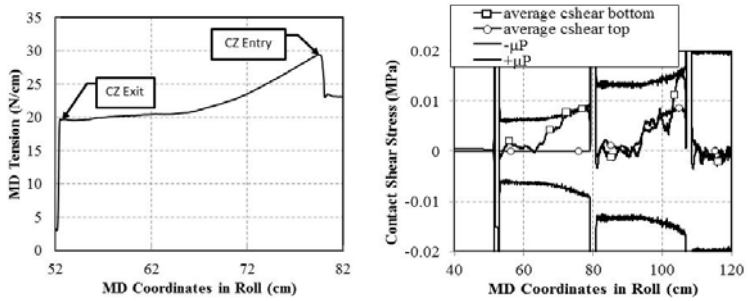

(a) (b)

Figure 19 – Determining the Final Value of the WOT (a) and Slippage of the Outer Laps (b) N=193 N/cm

CONCLUSIONS

The winding simulations have shown that the explicit finite element modeling method is a powerful tool for studying the contact mechanics of winding.

The simulations have shown how to connect the experience bases from winding all web types on both center and surface winders using one theory. Those who wind low in-plane modulus webs know that web tension affects the WOT whether a surface or a center winder is used and that nip load may have little impact. The simulations exhibited this behavior in Figure 14. Those who wind high in-plane modulus webs know that very little web tension enters WOT if rolls are surface wound but that when center winding much of the web tension will become WOT. They also know that nip load directly affects WOT at low nip loads but less so at high nip loads. These behaviors were exhibited by the simulations in Figure 11. All of these behaviors are controlled by the slippage in the nip contact zone. This slippage is limited by friction but driven by the contact shear stresses that develop in the web as it travels through the nip. These contact shear stresses will be affected by nip and wound roll diameter, web tension and nip load and web material properties. Young's modulus and the shear modulus have a large influence on WOT. Depending on the slippage induced by the nip roller the final value of the WOT may or may not occur in the outer lap of the winding roll. Pfeiffer deduced this in his early tests [3]. The simulations have shown that nip induced slippage for layers beneath the outer layer can be important too.

REFERENCES

1. Good, J.K., Pfeiffer, J. D., and Giachetto, R.M., "Losses in Wound-on-Tension in the Center Winding of Wound Rolls," Proceedings of the Web Handling Symposium, ASME Applied Mechanics Division, AMD, Vol. 149, 1992, pp. 1-12.
2. Pfeiffer, J. D., "Internal Pressures in a Wound Roll of Paper," TAPPI Journal, Vol. 49, No. 8, 1966, pp. 342-347.
4. Rand, T. and Ericsson, L. G., "Physical Properties of Newsprint Rolls during Winding," TAPPI Journal, Vol. 56, No. 6, 1973, pp. 153-156.
5. Pfeiffer, J. D., "Nip Forces and Their Effect on Wound-in Tension," TAPPI Journal, Vol. 60, No. 2, 1977, pp. 115-117.
6. Good, J. K. and Fikes, M. W. R., "Predicting the Internal Stresses in Center Wound Rolls with an Undriven Nip Roller," TAPPI Journal, Vol. 74, No. 6, 1991, pp. 101-109.
7. Hakiel, Z., "Nonlinear Model for Wound Roll Stresses," TAPPI Journal, Vol. 70, No. 5, 1987, pp. 113-117.
8. Good, J. K., "The Abilities & Inabilities of Wound Roll Models to Predict Winding Defects," Proceedings of the Eighth International Conference on Web Handling, Web Handling Research Center, Oklahoma State University, Stillwater, Oklahoma, 2005.
9. Steve, R. E., "The Effect of Nip Load on Wound-on-Tension in Surface Winding," M.S. Thesis, Oklahoma State University, Stillwater, OK, USA, 1995.
10. Good, J. K., Hartwig, J., and Markum, R., "A Comparison of Center and Surface Winding Using the Wound-in-Tension Method," Proceedings of the Fifth International Conference on Web Handling, Web Handling Research Center, Oklahoma State University, Stillwater, Oklahoma, 1999, pp. 87-104.
11. Jorkama, M. and von Hertzen, R., "Contact Mechanical Approach to the Winding Nip," Proceedings of the Fifth International Conference on Web Handling, Web Handling Research Center, Oklahoma State University, Stillwater, Oklahoma, 1999, pp. 39-49.
12. Jorkama, M. and von Hertzen, R., "Development of Web Tension in a Winding Nip," Proceedings of the Sixth International Conference on Web Handling, Web Handling Research Center, Oklahoma State University, Stillwater, Oklahoma, 2001, pp.123-134.
13. Jorkama, M. and von Hertzen, R., "The Mechanism of Nip Induced Tension in Winding," Journal of Pulp & Paper Science, Vo. 28, No. 8, 2002, pp. 280-284.
14. Panagiotopoulos, P. D., "A Nonlinear Programming Approach to the Unilateral Contact and Friction-Boundary Value Problem in the Theory of Elasticity," Ingenieur Archiv, Vol. 44, 1975, pp. 421-432.
15. Hibbitt, Karlsson, and Sorenson. Abaqus Theory Manual, Pawtucket, RI, USA, 1997.
16. Cheng, S. and Cheng, C. C., "Relation between E, ν, G and Invariants of the Elastic Coefficients for an Orthotropic Body," The Winter Annual Meeting of the American Society of Mechanical Engineers, , Applied Mechanics Division and the Materials Division, ASME, Dallas, Texas, Vol. 112, 1990, pp. 63-65.
17. ASTM D882-12: Test Method for Tensile Properties of Thin Plastic Sheeting, ASTM International, West Conshohocken, PA 19428-2959, USA.

18. ASTM D638-10: Standard Test Method for Tensile Properties of Plastics, ASTM International, West Conshohocken, PA 19428-2959, USA.
19. Physical-Thermal Properties of Mylar® Polyester Film, DuPont Teijin Films, Hopewell, VA 23860, USA.
20. Electrical Properties of Mylar® Polyester Film, DuPont Teijin Films, Hopewell, VA 23860, USA.